Clinical Study

Oncology

Oncology 2011;80:278–288
DOI: 10.1159/000328448

Received: November 9, 2010
Accepted after revision: February 23, 2011
Published online: July 7, 2011

Expression of Keratin 19 Is Related to High Recurrence of Hepatocellular Carcinoma after Radiofrequency Ablation

Kaoru Tsuchiya[a] Mina Komuta[b] Yutaka Yasui[a] Nobuharu Tamaki[a]
Takanori Hosokawa[a] Ken Ueda[a] Teiji Kuzuya[a] Jun Itakura[a]
Hiroyuki Nakanishi[a] Yuka Takahashi[a] Masayuki Kurosaki[a] Yasuhiro Asahina[a]
Nobuyuki Enomoto[c] Michiie Sakamoto[b] Namiki Izumi[a]

[a]Department of Gastroenterology and Hepatology, Musashino Red Cross Hospital, and [b]Department of Pathology, School of Medicine, Keio University, Tokyo, and [c]First Department of Internal Medicine, Yamanashi University School of Medicine, Yamanashi, Japan

Key Words
Hepatocellular carcinoma · Radiofrequency ablation · Recurrence · Keratin · Carcinogenesis · Needle biopsy · Hepatic progenitor cell

Abstract
Objective: Keratin (K) 19 positivity has been reported to be a useful predictive marker for recurrence in patients with hepatocellular carcinoma (HCC) who have undergone hepatic resection. We investigated the clinical usefulness of K19 positivity in patients who had received curative radiofrequency ablation (RFA). ***Methods:*** We retrospectively evaluated the clinicopathological features, including imaging and K19 expression, in 246 patients with HCC who were within the Milan criteria and had received curative RFA. Using a two-step insertion method, tumor biopsies were obtained just prior to RFA and were evaluated histologically. ***Results:*** Tumor seeding due to liver biopsy and RFA was not observed. Ten patients (4.1%) had K19-positive HCC. Imaging findings were similar between K19-positive and -negative HCC ($p = 0.187$). Nine out of 10 patients (90%) who had K19-positive HCC had recurrence of HCC after RFA, and intrahepatic recurrences were observed within 12 months in 6 out of 10 (60.0%). K19 positivity was a significant risk factor for recurrence ($p < 0.0001$) and early recurrence (<1 year after RFA; $p = 0.012$). K19 expression ($p = 0.016$) was an independent risk factor for tumor status exceeding the Milan criteria after RFA. ***Conclusion:*** Expression of K19 is related to high recurrence of HCC after curative RFA.

Introduction

Radiofrequency ablation (RFA) is regarded as an important treatment modality for hepatocellular carcinoma (HCC) [1–4], and its efficacy, especially for tumors <2 cm in diameter, is better than that of ethanol and nearly comparable to that of surgical resection [5]. In addition, RFA

Kaoru Tsuchiya and Mina Komuta contributed equally to this work.
Michiie Sakamoto and Namiki Izumi contributed equally to this work.

KARGER
Fax +41 61 306 12 34
E-Mail karger@karger.ch
www.karger.com

0030–2414/11/0804–0278$38.00/0

Accessible online at:
www.karger.com/ocl

Namiki Izumi, MD, PhD
Department of Gastroenterology and Hepatology
Musashino Red Cross Hospital
1-26-1 Kyonan-cho, Musashino-shi, Tokyo 180-8610 (Japan)
Tel. +81 422 32 3111, E-Mail nizumi@musashino.jrc.or.jp

is considered to be a bridge to liver transplantation because the prolonged waiting time for cadaveric livers leads to dropouts from the waiting list [6]. Tumor recurrence after curative RFA has been a problem, as it is after hepatic resection. Tumor size (>3 cm in diameter) [7], time after treatment (>1 year) [7], the number of HCC nodules [8] and hepatitis C virus (HCV) infection [8] have been reported to be risk factors for intrahepatic tumor recurrence after curative RFA. Moreover, primary technical failure is reported to be a risk factor for tumor progression beyond the Milan criteria after RFA [9].

Keratin (K) 19, which is considered to be a biliary/hepatic progenitor cell marker [10], has attracted attention as a useful predictive marker for detecting the more aggressive HCCs after curative resection, because tumors with K19 expression have a poorer prognosis [11, 12] and higher rates of recurrence [13, 14] and lymph node metastasis [12] than K19-negative HCC. In these previous studies, surgical specimens were investigated and K19 positivity was defined as expression in >5% of tumor cells [11–14].

As a result, one would expect that K19 expression might be a useful predictive marker for detecting HCC with a worse outcome after RFA, especially regarding tumor recurrence. To the best of our knowledge, the correlation between clinicopathological features and K19 expression has not been investigated in HCC patients treated by RFA. Therefore, we performed a clinicopathological study on 246 HCC cases treated with RFA and investigated the relationship between the K19 expression and recurrence and prognosis after treatment.

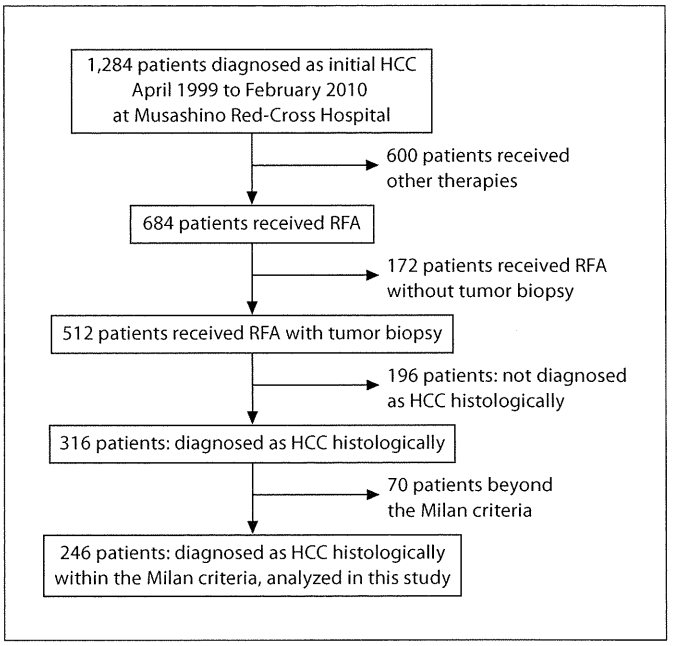

Fig. 1. Flow chart summarizing the patient selection for the study.

Methods

Patients

Between April 1999 and February 2010, 1,284 patients were admitted to the Musashino Red Cross Hospital for the first treatment of HCC. A total of 684 patients were treated with RFA as the initial therapy for HCC. Ablation therapy was chosen either because the patients were considered not to be suitable for resection (n = 323), when considering impairment of liver function, number and distribution of the tumors as well as cardiopulmonary dysfunction, or because they preferred ablation and provided informed consent (n = 361), despite surgery also being feasible. From the outset, 172 patients were excluded because RFA was performed without tumor biopsy. Therefore, 512 consecutive patients, on whom tumor biopsies had been performed before RFA, were included and we evaluated these specimens retrospectively. The result of retrospective analysis was that there were 57 patients with no residual samples, 119 patients with no tumorous lesion and 9 patients with no definitive histological diagnosis because of a small and/or fragmented specimen. The remaining specimens were diagnosed as HCC in 316 patients, as dysplastic nodule in 6 patients, as adenocarcinoma in 4 patients and as neuroendocrine tumor in 1 patient. Seventy patients were excluded, because their states of HCC were beyond the Milan criteria (≤3 cm and up to 3 nodules, or ≤5 cm and a single nodule). Therefore, 246 consecutive patients, on whom tumor biopsies had been performed before RFA and diagnosed as HCC retrospectively, were included in the study (fig. 1). The inclusion criteria for receiving RFA were as follows: total bilirubin concentration <3.0 mg/dl, platelet count $>3 \times 10^5/mm^3$, prothrombin activity >50% (approximately equal to an international normalized ratio of 1.5) and Child-Pugh score <8 points. Ascites were controlled by administration of diuretics before RFA. Patients with macroscopic vascular invasion or extrahepatic metastases were excluded. The criteria of the International Union against Cancer were used for TNM classification [15]. Written informed consent was obtained from all patients, and the study was approved by the ethics committee at Musashino Red Cross Hospital, in accordance with the Declaration of Helsinki.

Diagnosis of HCC

All the patients were diagnosed as having HCC on the basis of tumor markers and a combination of typical imaging findings on ultrasonography (US) and dynamic computed tomography (CT), according to the American Association for the Study of Liver Diseases and the Japan Society of Hepatology guidelines [1, 16]. When patients had 2 or 3 HCC nodules, a needle biopsy was taken from the main nodule. The histological diagnosis of HCC was based on the World Health Organization criteria [17].

For the evaluation of vascularity and Kupffer cell activity of the target nodule, CT during arteriography (CTHA) and CT dur-

ing arterioportography (CTAP) were performed in 188 (76.4%) patients, superparamagnetic iron oxide-enhanced magnetic resonance imaging (SPIO-MRI) was performed in 194 (78.8%) patients and gadolinium-ethoxybenzyl-diethylenetriamine pentaacetic acid magnetic resonance imaging (Gd-EOB-DTPA) was performed in 47 patients (19.1%), from March 2008. For triple-phase dynamic CT scans, arterial, portal and equivalent phases were 35, 70 and 150 s, respectively, after injection of contrast agent. Spiral CT scans were obtained from 3- to 5-mm-thick sections. Board-certified radiologists diagnosed HCC on the basis of typical patterns, such as an early-phase hyperattenuation area and late-phase hypoattenuation on dynamic CT. According to previous studies, the sensitivity of the diagnosis of HCC in CTHA/CTAP is higher than that of spiral CT. The diagnosis of HCC in CTHA/CTAP is hyperattenuation area in CTHA and hypoattenuation area in CTAP. It has been reported that the presence of Kupffer cells could be evaluated, and this was defined by a hyper-intensity area in the T2* image of SPIO-MRI as a typical imaging finding of HCC. Gd-EOB-DTPA MRI is a liver-specific contrast-enhanced agent, and hypointensity in the hepatobilliary phase is a typical imaging finding. We started to perform Gd-EOB-DTPA MRI instead of SPIO-MRI from March 2008, because it was reported that the sensitivity of Gd-EOB-DTPA MRI was superior to SPIO-MRI for the diagnosis of HCC.

Tumor Biopsy and RFA

There are 24 operators who participated in this study. They are specialized liver physicians who have great experiences in performing percutaneous ethanol injection for HCC, percutaneous tumor biopsy for liver tumor, percutaneous liver biopsy for hepatitis, percutaneous hepatobiliary drainage for obstructive jaundice, or percutaneous liver abscess drainage. A needle-guiding technique was used, consisting of an initial guided needle and a secondary outer needle (two-step insertion method). This method was reported by another center previously [18] and involves the initial insertion of a 21-gauge needle (Silux, Saitama, Japan) just adjacent to the tumor under real-time US guidance, and using this to insert a 14-gauge Daimon outer needle (Silux), also just adjacent to the tumor. After removal of the inner needle, an 18-gauge biopsy needle was inserted to obtain the tumor tissue sample. After removal of the biopsy needle, a 17-gauge cooled-tip electrode was inserted into the targeted tumor. The electrode, with a 2- or 3-cm exposed tip, was connected to a 480-kHz RF Generator (Radionics, Burlington, Mass., USA), which produces 200 W at 50 Ω of impedance [19, 20]. The equipment also allows the measurement of power output, tissue impedance and electrode tip temperature. A tip temperature of 10–20°C was maintained by infusion of chilled water through a peristaltic pump. After insertion of the electrode into the tumor, ablation was performed at 60 W for the 3-cm exposed tip and 40 W for the 2-cm exposed tip. The power was increased to 140 W at a rate of 10–20 W/min. When a rapid increase in impedance was observed during thermal ablation, the output was reduced. The duration of a single ablation was 12 min. After RF exposure, the pump was stopped and the temperature of the needle tip was measured. When the temperature of the electrode tip was >60°C, ablation was defined as being sufficient. When the target nodule was >2 cm in diameter, multiple needle insertions and ablations were performed in 1 nodule to achieve complete necrosis. A session was defined as a single intervention consisting of ≥1 ablations performed on ≥1 tumors at the same time. After completion of nodule ablation, the intrahepatic needle track was treated by thermocoagulation to avoid needle track seeding. Finally, a mixture of gelatin sponge particles (Gelfoam®; Upjohn, Kalamazoo, Mich., USA) was injected into the puncture route. All procedures were completed within 15–20 min. After each session of RFA, a dynamic CT scan (section thickness 5 mm) was performed to evaluate the efficacy of ablation. Complete ablation of HCC was defined as non-enhancement of the lesion, including the whole surrounding liver parenchyma. The ablative margin was shown as the boundary between the low density area as ablated area and the isodensity area as surrounding normal liver parenchyma. The residual portion of the tumor was treated by additional RFA within a few days of the post-treatment CT scan. Follow-up consisted of monthly serial measurements of tumor markers [α-fetoprotein (AFP) and des-γ-carboxy prothrombin (DCP)], US examination every 2 months and dynamic CT every 3 months. We checked various complications of RFA with conventional contrast-enhanced CT and blood examination at day 1 after RFA.

Tumor Recurrence

Recurrence of HCC was defined as an early enhancement area on dynamic CT, concomitant with late wash out. Two types of recurrence, local tumor progression and distant intrahepatic recurrence, were identified. Local tumor progression was defined as an enhancing area located adjacent to the ablated area [21], while distant intrahepatic recurrence referred to the appearance of a new tumor in the liver, distant from the ablated area. Early recurrence was defined as a recurrence within 12 months of the initial RFA.

Immunohistochemistry

Immunohistochemistry using antibodies against K19 (1:100, BA17, Dakocytomation, Glostrup, Denmark) was performed on paraffin-embedded sections from 246 needle biopsy specimens. The slides were reviewed by 2 independent pathologists (M. Komuta and M. Sakamoto). Expression of K19 was considered positive if >5% of tumor cells were stained according to the expected pattern of reactivity.

Statistical Analysis

Categorial variables were compared with the χ^2 test and continuous variables with the Mann-Whitney test; a p value <0.05 was considered statically significant. Continuous variables were expressed as the mean ± standard deviation. The imaging findings were compared with the χ^2 test between K19-positive and -negative patients. Overall survival was defined as the interval between treatment and death or the date of the last follow-up or the date of the most recent follow-up visit. Probability of recurrence-free survival was defined as the interval between treatment and the date of HCC recurrence.

Univariate analysis was performed to identify clinical and biological parameters (sex, age, etiology, prothorombin activity, albumin, bilirubin levels, Child-Pugh class, serum AFP level, serum DCP level) and tumor factors (size, number, tumor stage, tumor differentiation, K19 expression) predicting overall survival, recurrence-free survival and the interval beyond the Milan criteria.

Survival curves were computed according to the Kaplan-Meier method and compared by the log-rank test. All variables with a p value <0.05 were subjected to multivariate analysis by Cox's

Table 1. Comparison of clinicopathological features of patients (n = 246) with HCC with and without K19 expression

Features	K19 >5% (n = 10)	K19 ≤5% (n = 236)	p value
Mean age ± SD, years	70 ± 8	68 ± 8	0.541
Sex, male/female	2/8	146/90	0.016
Clinical and laboratory data			
Mean AFP, ng/ml	489 [52.1]	12 [16.2]	0.062
Mean DCP, mAU/ml	42 [25]	321 [22]	0.773
Child-Pugh score A/B	8/2	200/36	0.655
Total bilirubin, mg/dl	0.9 ± 0.5	0.8 ± 0.4	0.480
Albumin, g/dl	3.4 ± 0.7	3.6 ± 0.5	0.137
PT, %	97 ± 12	92 ± 15	0.375
Pathology			
Tumor size, mm	24 ± 7	22 ± 8	0.392
Tumor number	1.3 ± 0.7	1.2 ± 0.6	0.891
Vascular invasion, yes/no	0/10	0/236	
Tumor differentiation well/moderate/poor	0/8/2	108/126/2	<0.0001
TNM stage I/II	8/2	183/53	0.855
Lymph node involvement yes/no	0/10	0/236	
Metastasis, yes/no	0/10	0/236	
Major associated liver diseases			
HBsAg+	1 (10)	24 (10.1)	0.895
HCV Ab+	9 (90)	189 (80.1)	
ALD	0	8 (3.4)	
NASH	0	2 (0.8)	
Unknown etiology	0	13 (5.6)	

Figures in parentheses are percentages; figures in brackets are medians. PT = Prothrombin time; HBsAg = hepatitis B surface antigen; HCV Ab = HCV antibody; ALD = alcoholic liver disease; NASH = non-alcoholic steatohepatitis.

proportional hazards model to assess their value as independent predictors.

All statistical analyses were performed using StatView (version 5.0) software (Abacus Concepts, Berkeley, Calif., USA).

Results

Proportion of HCCs Expressing K19

The biopsy number was 272, and the median length of our biopsy specimens was 8.2 ± 4.0 mm. In 117 cases, the specimens were <1 cm, and ≥1 cm in 155 cases. Pathological diagnosis and K19 staining were practicable in all specimens <1 cm. Expression of K19 in >5% of tumor cells was observed in HCCs from 10 of 246 patients (4.1%). Two of the 10 HCCs (20.0%) were poorly differentiated, and 8 (80.0%) were moderately differentiated. None of the well-differentiated HCCs showed K19 positivity. Among the 10 patients with K19-positive HCCs, 2 had a HCC nodule >3 cm and 8 had HCC nodules ≤3 cm in diameter. The 8 HCC nodules with K19 positivity ≤3 cm in diameter were moderately (n = 7) and poorly differentiated HCCs (n = 1).

Table 2. Comparison of the image findings of patients with HCC with and without K19 expression

	K19 positive >5% (n = 10)	K19 negative (n = 236)	p value
CECT arterial phase high density	10/10	200/235	0.187
CTHA high density	7/7	159/181	0.326
CTAP low density	7/7	179/181	0.779
SPIO-MRI T2*	10/10	175/184	0.473
EOB-MRI			
Hepatobiliary phase low intensity	–	46/47	–

Clinicopathological Characteristics of Patients with HCC in Relation to Expression of K19

The clinicopathological characteristics of the patients in relation to K19 expression in HCCs are shown in table 1. The proportion of well-differentiated HCCs was significantly lower among K19-positive HCC patients ($p < 0.0001$). K19 expression was more frequent among female than among male patients ($p = 0.016$). There were no significant differences in age, clinical laboratory data, tumor size, number of tumor nodules, tumor stage in TNM classification or etiology between K19-positive and -negative HCC patients. There was no significant difference in tumor location (near the major vessels, bile ducts and organs) between K19-positive and -negative patients. The number of RFA sessions did not differ significantly between K19-positive and -negative HCC patients. Serum AFP before initial RFA was not evaluated in 1 patient.

Imaging Characteristics of HCCs in Relation to Expression of K19

Comparison of the various imaging findings, according to vascular profiling, and in relation to K19 expres-

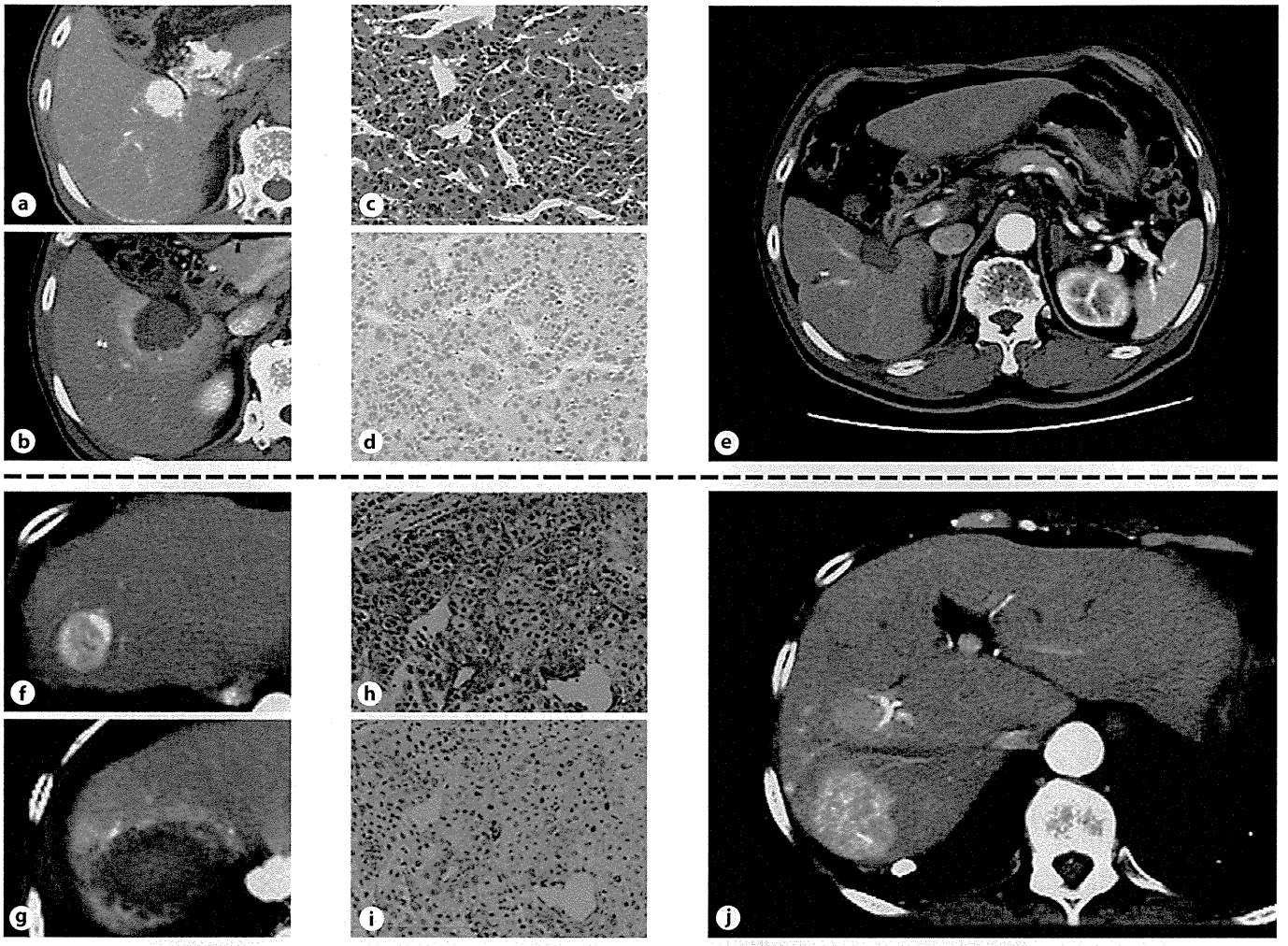

Fig. 2. a–e A patient with K19-negative HCC: a 70-year-old man with chronic hepatitis (anti-HCV positive). The HCC (25 mm in diameter, in segment 6) showed an early enhancement area by dynamic CT (**a**). Dynamic CT at 1 day after RFA (**b**). On histological investigation, the tumor showed moderately differentiated HCC on H&E staining (**c**), and K19 expression was negative in tumor cells (**d**). The HCC did not show early enhancement on dynamic CT 4 years and 10 months after curative RFA (**e**). **f–j** A patient with K19-positive HCC: a 72-year-old female with chronic hepatitis (anti-HCV positive). The HCC (25 mm in diameter, in segment 8) showed an early enhancement area by dynamic CT (**f**). CT 1 day after RFA (**g**). On histological investigation, the tumor showed moderately differentiated HCC on H&E staining (**h**), and K19-positive cells were seen in the tumor (**i**). Five months after RFA, the HCC showed intrahepatic recurrence beyond the Milan criteria (**j**).

sion, is shown in table 2. These imaging findings were consistent with the histological diagnosis, as determined by pretreatment needle biopsy.

All K19-positive HCCs showed typical HCC images, such as hypervascularity at the arterial phase, hypovascularity at the portal and equilibrium phases in dynamic CT, and hyperintensity at the T2* image in SPIO-MRI. There was no significant difference between K19-positive and -negative patients in terms of the imaging findings.

Recurrence of HCC after RFA

The median follow-up period was 34.0 months (range 65 days to 10.3 years). A recurrence of HCC was diagnosed at least once during the follow-up period in 156 patients (63.4%). The cumulative recurrence-free survival at 1, 3 and 5 years was 69.9, 26.6 and 12.2%, respectively. Among the 156 patients with recurrent HCC, 14 (8.9%) had local tumor progression and 142 (91.1%) had distant intrahepatic recurrences. Five of 14 patients (35%) who had local tumor progression had K19-positive HCC and

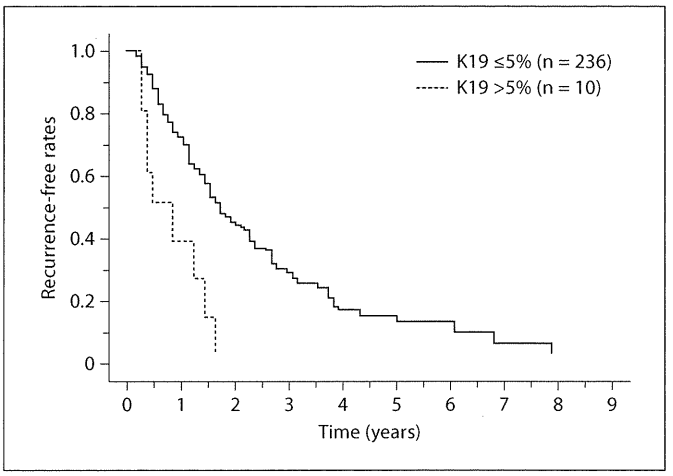

Fig. 3. The cumulative recurrence-free survival rate in patients with K19-positive (>5%) HCC was significantly lower than that in patients with K19-negative HCC (p = 0.0001).

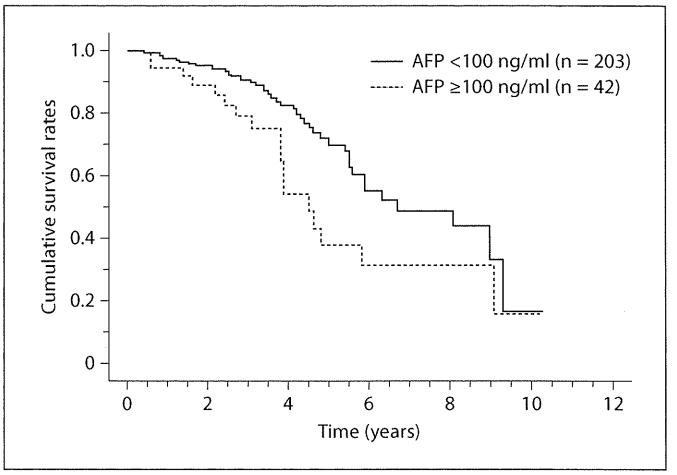

Fig. 4. The cumulative overall survival rate in patients with AFP ≥100 ng/ml was significantly lower than that in patients with AFP <100 ng/ml (p = 0.026).

3 of 5 patients with K19-positive HCC (60%) showed vascular invasion at the local tumor progression. Nine of 10 patients (90.0%) with K19-positive HCC had recurrences after initial treatment and 6 of 10 (60.0%) were detected within 1 year of initial curative RFA. On the other hand, 147 of 236 patients (62.2%) with K19-negative HCC had recurrences, and only 58 patients (24.5%) had recurrences within 1 year after RFA. There were no patients with K19-negative HCC who showed vascular invasion at the local tumor progression. Patients with K19-positive HCC were more likely to have an early recurrence of HCC (<1 year after RFA) than patients with K19-negative HCC (p = 0.012). The typical cases are shown in figure 2. The median recurrence-free survival in patients with K19-positive HCC was 194 days (range 93–635), while in patients with K19-negative HCC it was 446 days (range 65–2,978). Patients with K19-positive HCC had a significantly shorter recurrence-free survival than patients with K19-negative HCC (p = 0.0001) (fig. 3). The recurrence type, local tumor progression or distant intrahepatic recurrence differed between K19-positive and -negative patients. Local tumor progression was significantly higher in K19-positive patients than in K19-negative patients (p < 0.0001). Table 3 shows the results of univariate and multivariate analyses of prognostic factors for recurrence-free survival. In the multivariate analysis, K19 expression, the number of HCC nodules and total bilirubin ≥2 mg/dl were significant independent risk factors for HCC recurrence in all patients.

The percentage of distant metastasis and major portal invasion (VP3–4) was significantly higher in K19-positive than in K19-negative patients (p < 0.0001). Distal metastasis was detected in the lung (2 patients) and lymph node (1 patient), and major portal invasion was detected in 3 patients.

Risk Factors for Poor Prognosis

There was no patient who received liver transplantation in this study. Fifty-seven of 246 patients (23.1%) died during the follow-up period. The cause of death was progression of HCC in 37 patients, hepatic failure in 16 patients and causes unrelated to the liver in 4 patients. The overall survival rates for all patients were 97.2, 88.7 and 63.4% at 1, 3 and 5 years, respectively. A serum AFP level ≥100 ng/ml (p = 0.034), a total bilirubin level ≥2 mg/dl (p < 0.0001) and female sex (p = 0.018) were identified as risk factors for a poor prognosis in HCC in both univariate and multivariate analyses (table 4). Patients with high serum AFP levels (≥100 ng/ml) had significantly lower overall survival rates than patients with low serum AFP levels (p = 0.026) (fig. 4).

On the other hand, age (≥65 years), albumin concentration (≤3.5 g/dl), prothrombin time (≤70%), DCP (≥100 mAU/ml), tumor size, the number of HCC nodules and K19 expression were not significant risk factors for poor prognosis in the univariate analysis (table 4).

Table 3. Risk factors associated with recurrence-free survival in 246 patients with HCC after complete ablation by RFA

Risk factor	Univariate			Multivariate		
	RR	95% CI	p	RR	95% CI	p
Age <65 years	1.43	1.02–2.02	0.037	1.28	0.90–1.81	0.163
Sex, female	1.24	0.90–1.71	0.162			
Total bilirubin ≥2 mg/dl	2.50	1.02–6.25	0.034	2.70	1.08–6.66	0.032
Albumin ≤3.5 g/dl	1.12	0.81–1.56	0.492			
PT ≤70%	1.28	0.73–2.22	0.394			
AFP ≥100 ng/m	1.42	0.95–2.12	0.087			
DCP ≥100 mAU/ml	1.08	0.68–1.69	0.790			
Tumor size >3.0 cm	1.08	0.70–1.69	0.713			
2 or 3 tumor nodules	2.29	1.58–3.33	<0.0001	2.28	1.56–3.32	<0.0001
K19 positive (>5%)	3.57	1.75–7.14	0.0004	3.44	1.72–7.14	0.0005

RR = Risk ratio; CI = confidence interval; PT = prothrombin time.

Table 4. Risk factors associated with poor prognosis in 246 patients with HCC after complete ablation by RFA

Risk factor	Univariate			Multivariate		
	RR	95% CI	p	RR	95% CI	p
Age <65 years	1.19	0.68–2.09	0.527			
Sex, female	2.03	1.18–3.46	0.009	1.92	1.11–3.30	0.018
Total bilirubin ≥2 mg/dl	12.5	4.54–33.3	<0.0001	10.0	3.70–33.3	<0.0001
Albumin ≤3.5 g/dl	1.25	0.71–2.17	0.450			
PT ≤70%	1.49	0.59–3.84	0.674			
AFP ≥100 ng/ml	1.88	1.06–3.44	0.030	1.88	1.05–3.33	0.034
DCP ≥100 mAU/ml	1.06	0.53–2.12	0.880			
Tumor size >3.0 cm	1.12	0.44–1.78	0.730			
2 or 3 tumor nodules	1.23	0.67–2.26	0.492			
K19 positive (>5%)	1.29	0.46–3.57	0.632			

RR = Risk ratio; CI = confidence interval; PT = prothrombin time.

Risk Factors for Exceeding the Milan Criteria after RFA

Patients with K19-positive HCC exceeded the Milan criteria within 16.8 months. Multivariate analyses showed that K19 expression, high levels of DCP (≥100 mAU/ml), tumor number and total bilirubin ≥2 mg/dl were significant risk factors for tumor status exceeding the Milan criteria after curative RFA (table 5; fig. 5).

Complications

Most patients had mild pain or discomfort during RFA. Intraperitoneal hemorrhage and biloma were not seen in any patient. None of the patients developed dissemination of HCC, or skin or peritoneal metastases. There was no fatal complication.

Percentage of K19 Stain

We also analyzed another percentage of K19 stain (>1%). Thirteen of 246 patients had K19-positive (>1%) HCC and 12 of 13 patients with K19-positive (>1%) HCC had recurrences beyond the Milan criteria. Nine of 12 (75.0%) were detected with recurrence of HCC within 1 year of initial curative RFA. The final results were the same for K19 positivity (>5 and >1%, respectively). The

Table 5. Risk factors associated with exceeding the Milan criteria in 246 patients with HCC after complete ablation by RFA

Risk factor	Univariate			Multivariate		
	RR	95% CI	p	RR	95% CI	p
Age <65 years	1.63	1.08–2.45	0.018	1.17	0.75–1.83	0.463
Sex, female	1.16	0.78–1.72	0.457			
Total bilirubin ≥2 mg/dl	2.94	1.05–8.33	0.039	3.57	1.25–10.0	0.017
Albumin ≤3.5 g/dl	0.97	0.64–1.47	0.857			
PT ≤70%	0.89	0.41–1.96	0.763			
AFP ≥100 ng/ml	2.17	1.38–3.44	0.0008	1.56	0.96–2.50	0.077
DCP ≥100 mAU/ml	2.32	1.42–3.70	0.0007	2.08	1.26–3.44	0.004
Tumor size >3.0 cm	1.03	0.61–1.72	0.914			
2 or 3 tumor nodules	2.98	1.91–4.64	<0.0001	3.05	1.91–4.88	<0.0001
K19 positive (>5%)	3.70	1.81–7.69	0.0003	2.47	1.19–5.18	0.016

RR = Risk ratio; CI = confidence interval; PT = prothrombin time.

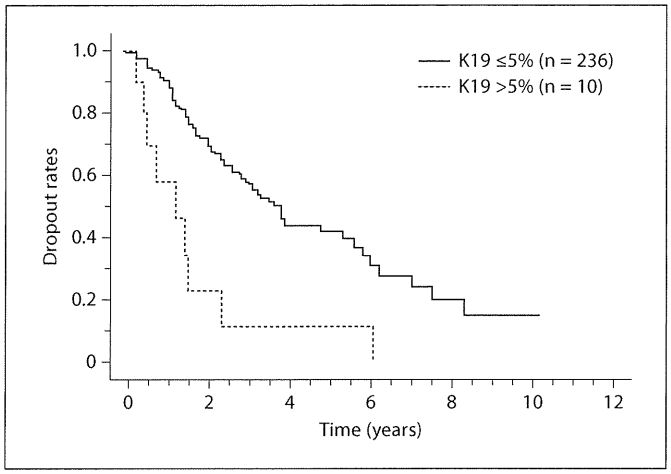

Fig. 5. The cumulative rate of exceeding the Milan criteria in patients with K19-positive HCC was significantly higher than that in patients with K19-negative HCC ($p < 0.0001$).

rate of recurrence and dropout from the Milan criteria were significantly higher in the patients with K19-positive (>1%) than in the patients with K19-negative HCC (data not shown).

Discussion

RFA therapy for HCC has been shown to achieve excellent results in appropriately selected patients [2–5]. However, recurrence of tumors is a serious impediment to improving the prognosis for patients treated with curative RFA. Therefore, several factors have been investigated as potential predictive markers for recurrence after curative RFA [7–9]. Recently, K19 was proposed as an independent prognostic factor for HCC [11–14]. However, these investigations were performed on surgically resected cases only and not on tumor biopsies. Although tumor biopsy is controversial because of potential complications such as tumor seeding [22], it would be beneficial to clinicians and patients to predict the individual tumor characteristics from a biopsy. Until now, the relationship between K19 expression and tumor recurrence after RFA treatment has not been assessed. Therefore, we have investigated the relationship between K19 expression in tumor biopsies and the clinicopathological findings in HCC. In this study, we investigated K19 expression in biopsy specimens taken just prior to the RFA session, and K19 expression (>5%) was demonstrated in 10 of 246 patients (4.1%). Because most of our patients were in early stage (within the Milan criteria) and 108 of 246 patients (43.9%) had well-differentiated HCC, the positive rate of K19 stain in our study was lower than that in surgical specimens.

We also analyzed another percentage of K19 stain (>1%) and the final results were the same for K19 positivity (>5 and >1%, respectively). K19 expression (>1%) was a statistically significant independent predictor for recurrence of HCC after RFA. Although the amount of tissue obtained by tumor biopsy is small compared to resected material, present data suggest that even biopsy can provide meaningful data on tumor recurrence irrespective of the percentage of K19 positivity (1 or 5%) (online sup-

plementary tables 1 and 2; for supplementary material see www.karger.com/doi/10.1159/000328448).

K19 positivity was not an independent predictor of the overall rate of survival, and serum AFP (≥100 ng/ml), total bilirubin (≥2 mg/dl) and female sex were significant independent predictors of survival. It is suggested that the level of total bilirubin affects the liver function of the patient, and liver function is one of the most important prognostic factors for survival of HCC patients.

The average age of our patients in this study was 68 ± 8 years, and no patients received liver transplantation in this study. However, liver transplantation is the most desirable treatment for HCC worldwide. Because of the prolonged waiting time for liver transplantation, RFA has been considered a safe and effective bridging therapy to liver transplantation. In addition, pretransplant RFA in patients with HCC has been considered for downstaging of HCC, thus improving the patient's survival [6, 7, 23]. In this study, K19 expression of HCC was a significant independent predictor for exceeding the Milan criteria ($p = 0.016$). In fact, 9 of 10 patients with K19-positive HCC exceeded the Milan criteria within 16.8 months. Therefore, if RFA is considered as a bridging therapy session prior to liver transplantation, it would be useful to obtain information on K19 expression in tumor tissue by performing a tumor biopsy before RFA. Therefore, careful observation for early detection of recurrence should be considered if K19-positive HCC patients are awaiting liver transplantation.

Compared to surgical specimens, biopsies taken prior to RFA may present some difficulties with regard to histological investigation. Needle biopsies of the nodules are less often indicated when typical vascular imaging of HCC is obtained, compared to hypovascular nodules. Needle tract seeding should also be considered. Needle biopsy has played an important role in making a diagnosis in the past. Recently, more reliance has been placed on the vascular imaging profile, because of its sensitivity and specificity without the risk of tumor dissemination. In addition, in comparison to recent advances in imaging, the information obtained from liver biopsy is lacking, as these only provide simple histological characterization, such as tumor differentiation [24]. Moreover, the positive predictive value of the vascular profile on dynamic imaging for diagnosis of HCC exceeds 95% [25]. Therefore, the current tendency is to consider needle biopsy as non-essential for diagnosis. However, in this study, K19-positive HCC showed exactly the same imaging findings as K19-negative HCC, suggesting that it is difficult to distinguish between these tumor types by imaging profile alone. In addition, K19-positive, moderately and/or poorly differentiated HCC showed similar cytological and structural abnormalities to K19-negative HCC, indicating that K19 positivity is unpredictable without staining. In figure 2, we present an impressive comparison of the features of K19-positive and -negative HCC, showing that, although the histology was similar, the prognosis for these patients was completely different. From these findings, it is clear that immunohistochemistry for K19 is the only way of demonstrating its positivity. Fortunately, staining for K19 on paraffin sections is common in diagnostic pathology, and it is not a problem to add this to routine hematoxylin and eosin (H&E) staining. Moreover, even for a general pathologist with no liver specialization, evaluating K19 expression should not be difficult, as long as care is taken not to count bile ducts, which may be associated with the remains of portal tracts. Taken together, these finding could indicate that it may be beneficial to check tumors for K19 positivity prior to RFA. Further research is warranted in larger groups to validate these findings and outweigh the potential additional clinical benefit compared to the potential risk of tract seeding during percutaneous biopsy.

Although biopsy has an important role in understanding the biological characteristics of HCC [26], tumor seeding by needle biopsy should be avoided. In practice, this is a major concern with needle biopsy of tumors. A review of tumor seeding following therapeutic procedures in HCC indicated that seeding occurred in 0–12.5% of cases (median 0.95%, mean 2.5%) [22]. As the time between biopsy and the treatment procedure was not specified, it is difficult to identify the factors that could have caused seeding. In the present study, tumor biopsies were performed just before RFA, using a needle-guiding technique, and tumor seeding was not observed. The same puncture line was used for both tumor biopsy and RFA, allowing complete ablation of the tumor using the tumor biopsy route. This may be one of the reasons it was possible in this study to biopsy the tumors without dissemination or bleeding. After treatment by RFA, the tumor cannot be investigated for histological features and K19 expression; therefore, we recommend taking a biopsy just before RFA for predicting tumor behavior using K19 expression. This would be valuable to both the clinician and the patient.

The mechanism of K19-positive HCC remains unclear. The facts that K19-positive cells are present in HCCs and that these positive cells form a spectrum suggest that K19-positive HCC may have originated from hepatic progenitor cells. These hepatic progenitor cells,

which are liver-specific adult stem cells, have potential stem cell features such as proliferation and differentiation. Once a tumor takes on these phenotypes, K19-positive HCC can still preserve these stem cell phenotypes. Therefore, this could be a possible reason why K19-positive HCC shows aggressive behavior in comparison with K19-negative HCC. In fact, previous publications and our study confirm these features [27].

In conclusion, we successfully evaluated the positivity of K19 in biopsy specimens. K19-positive HCCs showed significantly more frequent recurrence after curative RFA than K19-negative tumors and positive staining of K19 in the cytoplasm of HCC is closely associated with early intrahepatic recurrence (<1 year) and dropout from the Milan criteria. On imaging, K19-positive HCC showed only typical HCC findings and it was difficult to distinguish between K19-positive and -negative HCC. Taken together, these findings could indicate that >5% K19 positivity in tumor biopsy tissue is important for predicting tumor recurrence, which is not possible by imaging. Because of the high risk of tumor recurrence in K19-positive HCC, close observation for early detection of recurrence should be required.

Acknowledgments

We thank Hiroshi Suzuki, Satoshi Kusakari and Yuko Hashimoto for their excellent technical assistance, which was indispensable to this study.

This study was supported by grants from the Japanese Ministry of Welfare, Health, and Labor.

Disclosure Statement

The authors have nothing to disclose. They have no affiliation with the manufacturers of the drugs used in this study and have not received funding from the manufacturers to support this research.

References

1 Bruix J, Sherman M: Management of hepatocellular carcinoma. Hepatology 2005;42:1208–1236.

2 Tateishi R, Shiina S, Teratani T, Obi S, Sato S, Koike Y, Fujishima T, Yoshida H, Kawabe T, Omara M: Percutaneous radiofrequency ablation for hepatocellular carcinoma. An analysis of 1000 cases. Cancer 2005;103:1201–1209.

3 Shiina S, Teratani T, Obi S, Sato S, Tateishi R, Fujishima T, Ishikawa T, Koike Y, Yoshida H, Kawabe T, Omata M: A randomized controlled trial of radiofrequency ablation with ethanol injection for small hepatocellular carcinoma. Gastroenterology 2005;129:122–130.

4 Kudo M: Radiofrequency ablation for hepatocellular carcinoma: updated review in 2010. Oncology 2010;78:113–124.

5 Choi D, Lim HK, Rhim H, Kim YS, Lee WJ, Paik SW, Koh KC, Lee JH, Choi MS, Yoo BC: Percutaneous radiofrequency ablation for early-stage hepatocellular carcinoma as a first-line treatment: long-term results and prognostic factors in a large single-institution series. Eur Radiol 2007;17:684–692.

6 Lu DS, Yu NC, Raman SS, Lassman C, Tong MJ, Britten C, Durazo F, Saab S, Han S, Finn R, Hiatt JR, Busuttil RW: Percutaneous radiofrequency ablation of hepatocellular carcinoma as a bridge to liver transplantation. Hepatology 2005;41:1130–1137.

7 Mazzaferro V, Battiston C, Perrone S, Pulvirenti A, Regalia E, Romito R, Sarli D, Schavo M, Garbagnati F, Marchiano A, Spreafico C, Camerini T, Mariani L, Miceli R, Andreola S: Radiofrequency ablation of small hepatocellular carcinoma in cirrhotic patients awaiting liver transplantation: a prospective study. Ann Surg 2004;240:900–909.

8 Izumi N, Asahina Y, Noguchi O, Uchihara M, Kanazawa N, Itakura J, Himeno Y, Miyake S, Sakai T, Enomoto N: Risk factors for distant recurrence of hepatocellular carcinoma in the liver after complete coagulation by microwave or radiofrequency ablation. Cancer 2001;91:949–956.

9 Fernandes ML, Lin CC, Lin CJ, Chen WT, Lin SM: Risk of tumour progression in early-stage hepatocellular carcinoma after radiofrequency ablation. Br J Surg 2009;96:756–762.

10 Roskams T, De Vos R, Van Eyken P, Myazaki H, Van Damme B, Desmet V: Hepatic OV-6 expression in human liver disease and rat experiments: evidence for hepatic progenitor cells in man. J Hepatol 1998;29:455–463.

11 Yang XR, Xu Y, Shi GM, Fan J, Zhou J, Ji Y, Sun HC, Qiu SJ, Yu B, Gao Q, He YZ, Qin WZ, Chen RX, Yang GH, Wu B, Lu Q, Wu ZQ, Tang ZY: Cytokeratin 10 and cytokeratin 19: predictive markers for poor prognosis in hepatocellular carcinoma patients after curative resection. Clin Cancer Res 2008;14:3850–3859.

12 Zhuang PY, Zhang JB, Zhu XD, Zhang W, Wu WZ, Tan YS, Hou J, Tang ZY, Qin LX, Sun HC: Two pathologic types of hepatocellular carcinoma with lymph node metastasis with distinct prognosis on the basis of CK19 expression in tumor. Cancer 2008;112:2740–2748.

13 Uenishi T, Kubo S, Yamamoto T, Shuto T, Ogawa M, Tanaka H, Tanaka S, Kaneda K, Hirohashi K: Cytokeratin 19 expression in hepatocellular carcinoma predicts early postoperative recurrence. Cancer Sci 2003;94:851–857.

14 Durnez A, Verslype C, Nevens F, Fevery J, Aerts R, Pirenne J, Lesaffre E, Libbrecht L, Desmet V, Roskams T: The clinicopathological and prognostic relevance of cytokeratin 7 and 19 expression in hepatocellular carcinoma. A possible progenitor cell origin. Histopathology 2006;49:138–151.

15 Sobin LH, Fleming ID: TNM Classification of Malignant Tumors, fifth edition (1997). Union Internationale Contre le Cancer and the American Joint Committee on Cancer. Cancer 1997;80:1803–1804.

16 Kudo M, Okanoue T: Management of hepatocellular carcinoma in Japan: consensus-based clinical practice manual proposed by the Japan Society of Hepatology. Oncology 2007;72(suppl 1):2–15.

17 Hirohashi S, Ishak K, Kojiro M, Wanless I, Theise N, Tsukuma H: Tumours of the liver and intrahepatic bile ducts; in Hamilton SR, Aaltonen LA (eds): Pathology and Genetics of Tumours of the Digestive System. Lyon, IARC Press, 2000, pp 157–202.

18 De Baere T, Rehim MA, Teriitheau C, Deschamps F, Lapeyre M, Dromain C, Boige V, Dromain C, Boige V, Ducreux M, Elias D: Usefulness of guiding needles for radiofrequency ablative treatment of liver tumors. Cardiovasc Intervent Radiol 2006;29:650–654.
19 Lorentzen T: A cooled needle electrode for radiofrequency tissue ablation: thermodynamic aspects of improved performance compared with conventional needle design. Acad Radiol 1996;3:556–563.
20 Goldberg SN, Gazelle GS, Solbiati L, Rittman WJ, Mueller PR: Radiofrequency tissue ablation: increased lesion diameter with a perfusion electrode. Acad Radiol 1996;3:636–644.
21 Komorizono Y, Oketani M, Sako K, Yamasaki N, Shibatou T, Maeda M, Kohara K, Shigenobu S, Ishibashi K, Arima T: Risk factors for local recurrence of small hepatocellular carcinoma tumors after a single session, single application of percutaneous radiofrequency ablation. Cancer 2003;97:1253–1262.
22 Stigliano R, Marelli L, Yu D, Davies N, Patch D, Burroughs AK: Seeding following percutaneous diagnostic and therapeutic approaches for hepatocellular carcinoma. What is the risk and the outcome? Seeding risk for percutaneous approach of HCC. Cancer Treat Rev 2007;33:437–447.
23 Brillet PY, Paradis V, Brancatelli G, Rangheard AS, Consigny Y, Plessier A, Durand F, Belghiti J, Sommacale D, Vilgrain V: Percutaneous radiofrequency ablation for hepatocellular carcinoma before liver transplantation: a prospective study with histopathologic comparison. AJR Am J Roentgenol 2006;186:S296–S305.
24 Pawlik TM, Gleisner AL, Anders RA, Assumpcao L, Maley W, Choti MA: Preoperative assessment of hepatocellular carcinoma tumor grade using needle biopsy: implications for transplant eligibility. Ann Surg 2007;245:435–442.
25 Bruix J, Sherman M, Llovet JM, Beaugrand M, Lencioni R, Burroughs AK, Christensen E, Pagliaro L, Colombo M, Rodes J, EASL Panel of Experts on HCC: Clinical management of hepatocellular carcinoma. Conclusions of the Barcelona-2000 EASL conference. European Association for the Study of the Liver. J Hepatol 2001;35:421–430.
26 Rockey DC, Caldwell SH, Goodman ZD, Nelson RC, Smith AD: Liver biopsy. Hepatology 2009;49:1017–1044.
27 van Sprundel RG, van den Ingh TS, Spee B: Keratin 19 marks poor differentiation and a more aggressive behavior in canine and human hepatocellular tumours. Comp Hepatol 2010;9:4.

J Gastroenterol (2011) 46:1238–1248
DOI 10.1007/s00535-011-0437-3

ORIGINAL ARTICLE—LIVER, PANCREAS, AND BILIARY TRACT

Evaluation of liver fibrosis by transient elastography using acoustic radiation force impulse: comparison with Fibroscan®

Hirotoshi Ebinuma · Hidetsugu Saito · Mina Komuta · Keisuke Ojiro · Kanji Wakabayashi · Shingo Usui · Po-sung Chu · Rumiko Umeda · Yuka Ishibashi · Tetsurou Takayama · Masahiro Kikuchi · Nobuhiro Nakamoto · Yoshiyuki Yamagishi · Takanori Kanai · Kiyoshi Ohkuma · Michiie Sakamoto · Toshifumi Hibi

Received: 22 December 2010 / Accepted: 8 June 2011 / Published online: 21 July 2011

Abstract
Background Accurate evaluation of liver fibrosis in patients with chronic liver damage is required to determine the appropriate treatment. Various approaches, including laboratory tests and transient elastography, have been used to evaluate liver fibrosis. Recently, transient elastography with acoustic radiation force impulse (ARFI) has been developed and applied with conventional ultrasonography. The aim of this study was to evaluate the clinical utility of transient elastography with ARFI and to compare the results with this method and those of the Fibroscan® procedure.
Methods One hundred and thirty-one patients with liver damage, who underwent liver biopsy at our department, were enrolled prospectively in this study. Elastography with ARFI (applied with ACUSON S2000®), and Fibroscan® was performed at the same time as liver biopsy. These measurements were compared with histological findings in liver biopsy specimens, and measurement accuracy was evaluated by receiver-operating characteristic analysis.
Results Elastography values with both procedures were significantly correlated with the stages of liver fibrosis and there was little difference in the results obtained using the 2 procedures. The accuracy of differential diagnosis between no fibrosis at F0 and more than F1 stage was insufficient with ARFI, but this procedure was sufficient for diagnosing advanced fibrosis. The accuracy of ARFI was almost equivalent to that of the Fibroscan® method. Moreover, both ARFI and Fibroscan® values increased in proportion to the severity of hepatic inflammation when fibrosis stage is low, but not in proportion to the severity of steatosis.
Conclusions Transient elastography with ARFI is simple, non-invasive and useful for diagnosing the stage of fibrosis in chronic liver disease. The utility of ARFI was almost equivalent to that of the Fibroscan® method.

Keywords Transient elastography · Acoustic radiation force impulse · Liver stiffness · Non-invasive · Fibrosis

Abbreviations

ARFI	Acoustic radiation force impulse
HCC	Hepatocellular carcinoma
US	Ultrasonography
ROI	Region of interest
ROC	Receiver operating characteristic
AUROC	Area under ROC curve

Introduction

The development of fibrotic changes in the liver is associated with the progression of chronic liver diseases and is

H. Ebinuma · H. Saito · K. Ojiro · K. Wakabayashi · S. Usui · P. Chu · R. Umeda · Y. Ishibashi · T. Takayama · M. Kikuchi · N. Nakamoto · Y. Yamagishi · T. Kanai · T. Hibi
Division of Gastroenterology and Hepatology, Department of Internal Medicine, School of Medicine, Keio University, Tokyo, Japan

H. Saito (✉)
Department of Internal Medicine, School of Medicine and Faculty of Pharmacy, Keio University, 35 Shinanomachi, Shinjuku-ku, Tokyo 160-8582, Japan
e-mail: hsaito@sc.itc.keio.ac.jp

M. Komuta · M. Sakamoto
Department of Pathology, School of Medicine, Keio University, Tokyo, Japan

K. Ohkuma
Department of Diagnostic Radiology, School of Medicine, Keio University, Tokyo, Japan

the result of hepatic wound healing following the continuous destruction of hepatocytes. In recent work, hepatic fibrosis has been viewed not as a static lesion, but as a lesion that may improve or worsen, dependent on the activity of these diseases [1]. The stage of fibrosis in chronic viral hepatitis correlates with the risk of hepatocarcinogenesis and decompensated cirrhosis, and successful anti-viral therapy results in decreases in the fibrosis stage and in the risk of the development of hepatocellular carcinoma (HCC).

Although needle biopsy is the gold standard for the evaluation of liver fibrosis in living patients [2], the procedure may be subject to sampling error, because only 1/50,000 of the entire liver is evaluated [3, 4], and the procedure may lead to complications including death [5]. Histological diagnosis is a subjective procedure and inter-observer and intra-observer differences in diagnoses sometimes occur [3]. Moreover, liver fibrosis occurs continuously, not stepwise, and fibrosis progresses finally to F4 stage. Laparoscopy is a macroscopic approach to the evaluation of liver fibrosis, but a recent report documented several cases in which the laparoscopic aspects and histological findings were disparate [6]. These findings suggest that an objective evaluation of liver fibrosis is required.

Transient elastography has been applied in the field of hepatology. The clinical usefulness of the Fibroscan® (EchoSens, Paris, France) device has been widely replicated following the first report of the technique by Sandrin et al. [7]. The Fibroscan® module uses a system in which external mechanical excitation is channeled into the liver and shear wave speeds are measured using ultrasonography (US). The elasticity of the liver is reduced by the accumulation of fibrosis, so that the measurement of elasticity correlates to the degree of liver fibrosis. We first reported the usefulness of Fibroscan® for measuring liver stiffness in Japanese patients with chronic hepatitis C [8]. In contrast, the technology of acoustic radiation force impulse (ARFI) is based on the principle of the mechanical excitation of tissue by short-duration acoustic pulses. This technology was initially used for imaging different materials in soft tissues clearly by producing shear waves with ARFI. Fahey et al. [9] first reported the efficacy of ARFI for detecting and monitoring the progression of human HCC and renal cancers. In 2008, Palmeri et al. [10] first described transient elastography of the human liver tissue using ARFI technology. Recently ARFI-assisted transient elastography was made commercially available in a US apparatus; this advance made it possible to measure the stiffness in a region of interest (ROI) chosen by the operator [11].

The aim of this study was to evaluate the clinical utility of transient elastography measured using ARFI technology and to compare these results and those obtained using the Fibroscan® method with the gold standard for the measurement of liver fibrosis in Japanese patients with various forms of liver injury.

Patients and methods

Enrolled patients

One hundred and thirty-one patients with liver damage, who underwent percutaneous liver needle biopsy at our department from October 2008 to October 2009, were enrolled prospectively in this study after receiving documentation of the purpose and methods and providing consent to participate.

Measurement of liver stiffness

Liver stiffness was measured by ARFI, using an ACUSON S2000® (Mochida Siemens Medical Systems, Tokyo, Japan), which enabled convenient and simple measurement of liver elasticity during US; and by Fibroscan® (Echo-Sens). Both procedures were performed at the same time as the percutaneous liver needle biopsy procedure, and the operators were blinded to the histology results. Measurement of liver stiffness using the ACUSON S2000® was performed by simply pushing a button during observation of the ROI in the liver. The elasticity was shown as the speed of the shear wave (m/s) proceeding vertically from the site where ARFI was produced in the liver. Elastography with the ACUSON S2000® was performed at two sites: the right lobe from the intercostal space at a depth of 3 cm from the surface and the left lobe from the median line at a depth of 2 cm from the surface. Liver elasticity was measured 10 times per patient and the median value was recorded. Elasticity was measured simultaneously using the Fibroscan® procedure. Measurement with the Fibroscan® was performed for the right lobe from the intercostal space and the measurement was determined automatically in any 2-cm region in the liver at a depth 2.5–6.5 cm from the surface. The measurement of a patient's liver was performed 10 times and the median value was shown automatically in the window.

We investigated the correlation between the stage of liver fibrosis and the results of elastography measured with the ACUSON S2000® and Fibroscan®. The stage of liver fibrosis was determined according to the METAVIR or New-Inuyama staging by experts in liver pathology [12]. In some samples, the stage of steatohepatitis was also assessed according to Brunt's classification [13]. Biopsy samples less than 1.5 cm in length were excluded.

Blood chemistry and hematologic tests

Blood chemistry and hematologic tests were carried out using conventional autoanalyzers at the same time as the liver stiffness was measured. Data associated with liver stiffness were selected and the results were compared between ARFI and Fibroscan®.

Statistical analysis

Elastography data for each fibrosis stage were calculated and expressed as means ± standard deviation. Correlation between elastography values and fibrosis stage was determined by Kruskal–Wallis analysis and the Jonckheere–Terpstra test. Correlation between the elastography values of ARFI and Fibroscan® was determined by the Pearson product-moment correlation coefficient. A receiver-operating characteristic (ROC) curve was used to determine the best cut-off value for differentiating each F stage and the efficacy was analyzed based on the area under the ROC curve (AUROC) and the likelihood ratio test. The AUROC values of ARFI and Fibroscan® were compared by the χ^2 test. These analyses were performed with SAS computer program software (SAS Institute, Cary, NC, USA).

Results

Patient characteristics

Liver stiffness in the 131 patients with liver damage was measured by ARFI and Fibroscan® at the same time as their percutaneous liver biopsies were performed. The clinical details of these patients are given in Fig. 1. Among the 131 patients, 18 exhibited acute liver damage and were excluded from some of the analyses because it was likely that severe inflammation of the liver would have affected the elastography measurements [14, 15]. Patients with an acute clinical course with the following conditions were included in the analysis : 1 with acute hepatitis A, 1 with acute hepatitis C, 2 with acute hepatitis E, 1 with acute hepatitis due to Epstein-Barr (EB) virus infection, 2 with acute-onset drug-induced liver injury, 2 with acute-onset autoimmune hepatitis, and 9 with acute liver injury of unknown etiology. Among these 18 patients, 2 presented with fulminant liver failure (1 with viral hepatitis and 1 with hepatitis of unknown etiology) and were suspected to have severe fibrosis as a result of severe acute hepatitis. Of the remaining patients, 59 had chronic viral hepatitis (4 were hepatitis B virus-positive and 55 were hepatitis C virus-positive) and 54 were without chronic viral infection (10 had autoimmune hepatitis; 5,primary biliary cirrhosis; 1, primary sclerosing cholangitis; 11, alcoholic liver damage including cirrhosis; 20, non-alcoholic steatohepatitis including cirrhosis; and 7, unknown etiology). The background characteristics of the patients enrolled in the study are shown in Table 1. ARFI measurement was possible in all of these patients; however, Fibroscan® measurement was not possible in 4 patients because of thick subcutaneous fat tissue ($n = 3$) and liver atrophy ($n = 1$).

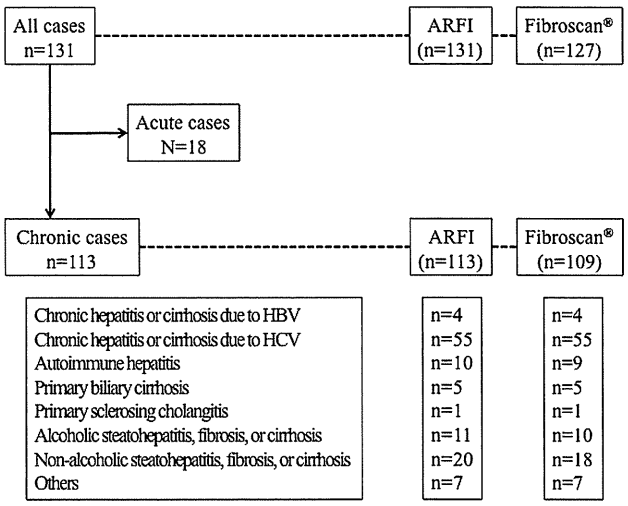

Fig. 1 Characteristics of the patients enrolled in this study. One hundred and thirty-one patients who consented to percutaneous liver biopsy were enrolled. The measurement of liver stiffness by acoustic radiation force impulse (*ARFI*) was possible for all patients, but measurement by Fibroscan® failed for 4 patients because of thick subcutaneous fat tissue ($n = 3$) and liver atrophy ($n = 1$). *HBV* hepatitis B virus, *HCV* hepatitis C virus

Correlation between elastography values and fibrosis stage

Liver stiffness was measured by ARFI with the ACUSON S2000® in the left and right lobes of the liver and by the Fibroscan® method in the right lobe of the liver. ARFI values were determined as velocity (m/s) and Fibroscan® values were determined as elasticity (kPa). Values for the three sets of measurements (ARFI-R (right), ARFI-L (left), and Fibroscan®) increased in proportion to increases in the fibrosis stage (Fig. 2a). The respective mean values for fibrosis stages F0, F1, F2, F3, and F4 were 1.36 ± 0.42, 1.36 ± 0.38, 1.64 ± 0.50, 2.28 ± 0.57, and 2.31 ± 0.78 m/s with ARFI-R ($p < 0.0001$ by Kruskal–Wallis analysis and Jonckheere–Terpstra test), 1.64 ± 0.38, 1.56 ± 0.42, 2.10 ± 0.44, 2.47 ± 0.58, and 2.70 ± 0.68 m/s with ARFI-L ($p < 0.0001$); and 8.4 ± 5.6, 8.4 ± 4.6, 13.1 ± 8.4, 21.1 ± 12.3, and 27.7 ± 16.2 kPa with Fibroscan® ($p < 0.0001$) (Fig. 2a). The Fibroscan® values of patients with acute liver damage were found to be higher than those of patients with chronic liver damage; therefore, we analyzed the data

Table 1 Background characteristics of the patients enrolled in this study

Etiology	Age (years)	Gender (M/F)	Fibrosis (F0/1/2/3/4)	Platelets ($\times 10^3/\mu l$)	Albumin (g/dl)	ALT (IU/l)
Acute ($n = 18$)	57.5 ± 18.0	10/8	9/7/1/1/0	217.1 ± 108.2	3.6 ± 0.6	1059 ± 1290
Chronic ($n = 113$)	64.3 ± 14.3	59/54	10/58/11/16/18	171.7 ± 67.2	4.0 ± 0.5	91 ± 131
CH-B ($n = 4$)	52.3 ± 16.2	4/0	0/2/1/0/1	227.8 ± 91.7	4.2 ± 0.3	296 ± 357
CH-C ($n = 55$)	69.2 ± 12.1	31/24	0/32/6/10/7	148.4 ± 60.2	3.9 ± 0.5	57 ± 41
AIH ($n = 10$)	56.5 ± 13.7	1/9	2/4/1/1/2	173.9 ± 52.3	3.8 ± 0.7	233 ± 290
PBC/PSC ($n = 6$)	54.7 ± 14.6	2/4	1/5/0/0/0	221.5 ± 27.6	4.2 ± 0.1	36 ± 28
ASH/NASH ($n = 31$)	63.7 ± 13.0	16/15	3/13/3/5/7	179.6 ± 61.5	4.2 ± 0.5	84 ± 58
Others ($n = 7$)	54.1 ± 20.5	5/2	4/2/0/0/1	242.3 ± 90.6	3.9 ± 0.3	109 ± 143
Total ($n = 131$)	63.3 ± 14.9	69/62	19/62/13/17/18	177.9 ± 75.3	4.0 ± 0.5	224 ± 587

Acute acute liver injury, *Chronic* chronic liver injury, *CH-B* chronic hepatitis B, *CH-C* chronic hepatitis C, *AIH* autoimmune hepatitis, *PBC* primary biliary cirrhosis, *PSC* primary sclerosing cholangitis, *ASH* alcoholic steatohepatitis, *NASH* non-alcoholic steatohepatitis, *ALT* alanine aminotransferase

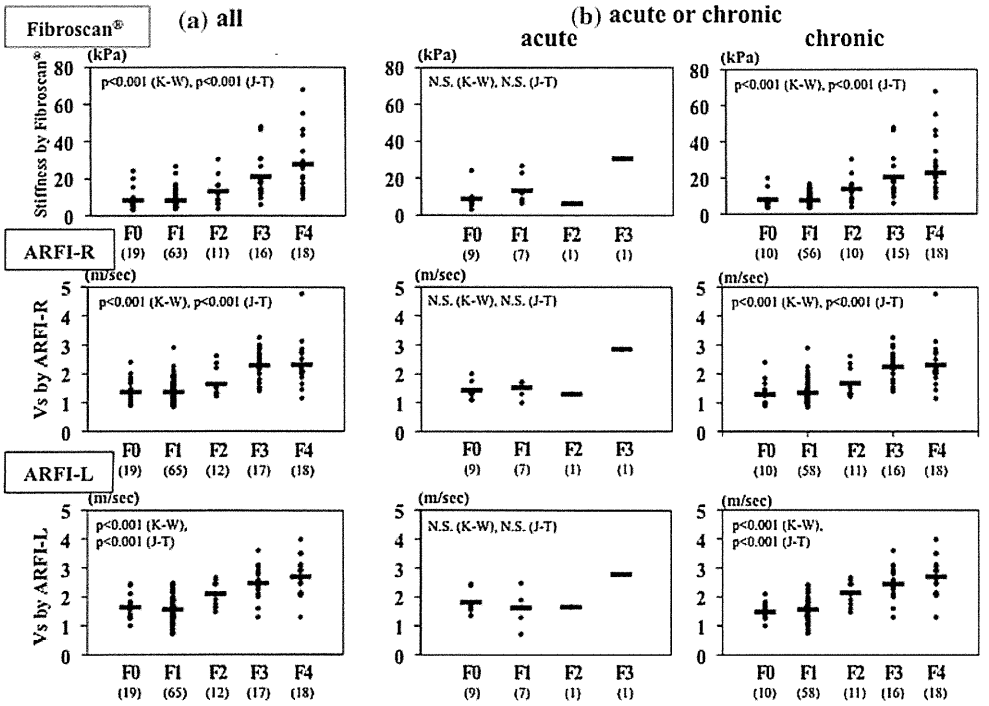

Fig. 2 Correlation between elastography values and fibrosis stage. **a** All patients enrolled in this study, **b** patients stratified by acute and chronic liver injury. The *horizontal lines* indicate the average values of liver stiffness for each stage. Values obtained using the Fibroscan® method increased in proportion to the extent of fibrosis in patients with chronic liver injury ($p < 0.0001$ in chronic liver injury as determined by Kruskal–Wallis (*K-W*) analysis and the Jonckheere–Terpstra (*J-T*) test; not significant (*N.S.*) in patients with acute liver injury). Similar results were seen with acoustic radiation force impulse (right) (*ARFI-R*) ($p < 0.0001$ in chronic liver injury, not significant in acute liver injury) and ARFI (left) (*ARFI-L*) ($p < 0.0001$ in chronic liver injury, not significant in acute liver injury)

separately for patients with acute liver damage and those with chronic liver damage. As reported previously, there was no correlation between the elastography values and the fibrosis stages in patients with acute liver damage (Fig. 2b, left). On the contrary, all these values increased significantly in parallel with the increase in fibrosis stage in patients with chronic liver damage. The respective mean values at fibrosis stages F0, F1, F2, F3, and F4 were 1.29 ± 0.51, 1.35 ± 0.39, 1.68 ± 0.52, 2.24 ± 0.57, and 2.31 ± 0.78 m/s with ARFI-R ($p < 0.0001$); 1.48 ± 0.33, 1.56 ± 0.41, 2.14 ± 0.43, 2.45 ± 0.59, and 2.70 ± 0.68 m/s with ARFI-L ($p < 0.0001$); and 8.0 ± 5.4, 7.7 ± 3.6, 13.9 ± 8.5, 20.5 ± 12.5, and 27.7 ± 16.2 kPa with Fibroscan® ($p < 0.0001$) (Fig. 2b, right).

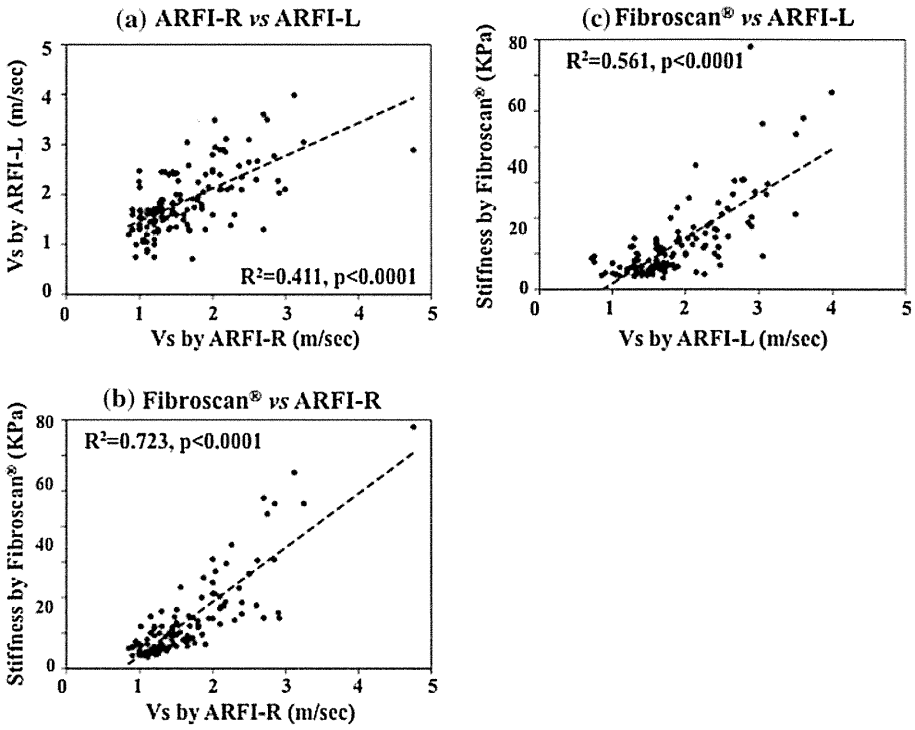

Fig. 3 Correlations between values obtained using the two transient elastography measurement methods. A significant correlation was observed between ARFI-R and ARFI-L values **a** ([ARFI-R] = 0.63[ARFI-L] + 0.45, $R^2 = 0.411$, $p < 0.0001$ by Pearson product-moment correlation coefficient], between ARFI-R and Fibroscan® values **b** ([Fibroscan®] = 15.18[ARFI-R] − 11.54, $R^2 = 0.723$, $p < 0.0001$), and between ARFI-L and Fibroscan® values **c** ([Fibroscan®] = 12.59[ARFI-L] − 10.90, $R^2 = 0.561$, $p < 0.0001$)

We also compared the values of these measurements between patients with acute liver damage and those with chronic liver damage at the same stage of fibrosis (F0 or F1). The values in patients with acute liver damage were greater than those in patients with chronic liver damage, but the only significant difference was for Fibroscan® at stage F1 (data not shown).

Correlation between ARFI and Fibroscan® measurements

Correlations between ARFI-R, ARFI-L, and Fibroscan® values were analyzed. As shown in Fig. 3, significant correlations were evident between ARFI-R and ARFI-L ($R^2 = 0.4109$, $p < 0.0001$ by Pearson product-moment correlation coefficient), ARFI-R and Fibroscan® ($R^2 = 0.7227$, $p < 0.0001$), and ARFI-L and Fibroscan® values ($R^2 = 0.5609$, $p < 0.0001$).

Correlation between values of elastography, blood chemistry, and hematologic test

Because elastography values would be expected to be greater in patients with acute liver damage, the following analyses were performed only for patients with chronic liver damage. In these analyses, ARFI values are represented by ARFI-R values.

We examined the correlation between values of elastography and laboratory tests that are related to liver fibrosis. As shown in Table 2, both Fibroscan® and ARFI-R values were inversely correlated with platelet counts (Fibroscan®: $p < 0.0001$, $R^2 = 0.247$; ARFI-R: $p < 0.0001$, $R^2 = 0.192$ by Pearson product-moment correlation coefficient). In addition, the elastography values were correlated with serum albumin, cholesterol, total bilirubin, γ-globulin level, prothrombin time (international rate), type IV collagen 7S fragment, and hyaluronate (Table 2); the correlations of serological liver fibrosis markers, type IV collagen 7S fragment and hyaluronate, were stronger than those of other

Table 2 Correlation of elastography values with results of blood chemistry and hematology tests (indicated by R^2, * $p < 0.05$ by Pearson product-moment correlation coefficient)

	Fibroscan® ($n = 127$)	ARFI-R ($n = 131$)
Platelet count	0.247*	0.192*
Serum albumin	0.306*	0.232*
AST	0.011	0.019
ALT	0.001	0.003
γ-GTP	0.010	0.031
Total cholesterol	0.130*	0.067*
Total bilirubin	0.235*	0.226*
γ-Globulin	0.086*	0.049*
Prothrombin time	0.173*	0.107*
Type IV collagen 7S	0.575*	0.512*
Hyaluronic acid	0.370*	0.351*

AST aspartate aminotransferase, *γ-GTP* gamma-glutamyl transpeptidase, *ARFI-R* acoustic radiation force impulse (right)

markers tested, and the correlation of Fibroscan® and ARFI-R values were similar.

Overall accuracy of elastography in differentiation between stages of fibrosis

Efficacy was analyzed based on the AUROC, and the best cut-off value for differentiating each F stage was determined (Fig. 4; Table 3a). The accuracy of ARFI-R and Fibroscan® in the diagnosis between F0 and F1–4 was 0.690 and 0.724, respectively. The cut-off values that differentiated between F0 and F1–4 by ROC analysis were 6.2 kPa for Fibroscan® and 1.02 m/s for ARFI-R. For the diagnosis between F0–1 and F2–4 or greater fibrosis stage, the accuracy was 0.891 for Fibroscan® and 0.871 for ARFI-R, and the cut-off values between F0–1 and F2–4 were 9.1 kPa and 1.30 m/s, respectively. In the diagnosis between F0–2 and F3–4 or greater fibrosis stage, accuracy was 0.908 for Fibroscan® and 0.890 for ARFI-R, and the cut-off values between F0–2 and F3–4 were 11.6 kPa and 1.65 m/s, respectively. In the diagnosis of F4 fibrosis stage, accuracy was 0.888 for Fibroscan® and 0.817 for ARFI-R, and the cut-off values between F0–3 and F4 were 14.3 kPa and 1.88 m/s, respectively. The likelihood ratio of a positive test between F0 and F1–4 was low (1.44 for Fibroscan® and 2.25 for ARFI-R), but the likelihood ratio for differentiating between fibrosis stages of F1 and greater were sufficient. Thus, both elastography methods differentiated F1 and greater accurately, but they lacked accuracy in differentiating between F0 and F1.

There were no significant differences in the AUROC values for ARFI-R and Fibroscan® at each fibrosis stage ($p = 0.748$ at F0 and F1–4, $p = 0.512$ at F0–1 and F2–4, $p = 0.344$ at F0–2 and F3–4, $p = 0.908$ at F0–3 and F4, by χ^2 analysis).

Differences in the accuracy of elastography according to the cause of liver damage

This study included patients with liver damage of various causes. Because the pattern of hepatic fibrosis differed between patients with chronic viral hepatitis and those with steatohepatitis (such as alcoholic liver diseases or non-alcoholic steatohepatitis), we examined whether the accuracy of 2 elastography methods was different between patients with chronic viral hepatitis (hepatitis B and C viruses; viral) and those without viral hepatitis (non-viral). Elastography values increased in parallel with the degree of increase in fibrosis in patients with viral hepatitis (viral) and in those without viral hepatitis (non-viral) (Fig. 5). The accuracy of Fibroscan® and ARFI-R for the diagnosis of fibrosis determined by ROC analysis was higher in the patients with viral etiology than in those with non-viral etiology, but both methods were able to distinguish the

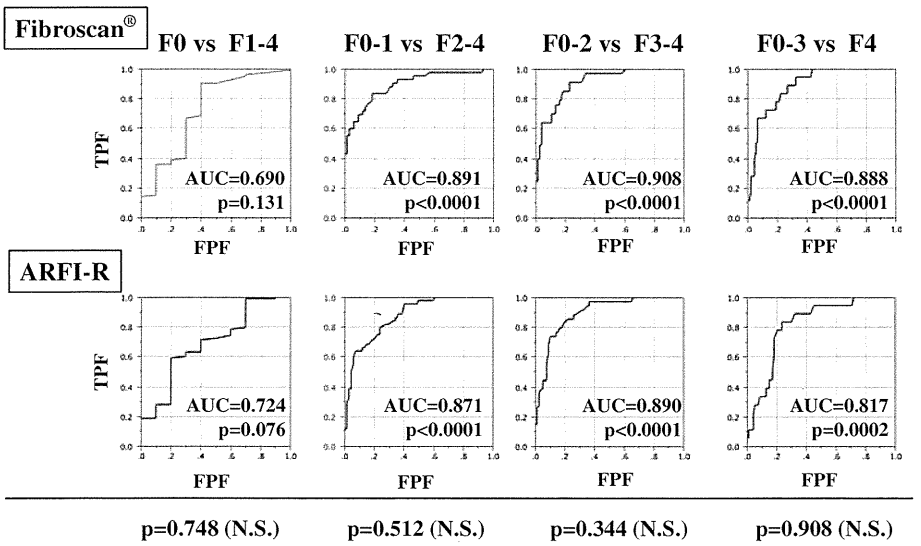

Fig. 4 Accuracy of elastography in differentiating between different stages of fibrosis. The accuracy of differential diagnosis between stage F0 and F1–4 was unsatisfactory with both the Fibroscan® and the ARFI-R methods (area under receiver-operating characteristic curve [AUROC] = 0.690 for Fibroscan®, $p = 0.131$ by χ^2 analysis; AUROC = 0.724 or ARFI-R, $p = 0.076$). However, the accuracy of both methods was sufficient for the diagnosis of stages greater than F2 (Fibroscan®, AUROC = 0.891, $p < 0.0001$; ARFI-R, AUROC = 0.871, $p < 0.0001$), F3 (Fibroscan®, AUROC = 0.908, $p < 0.0001$, ARFI-R, AUROC = 0.890, $p < 0.0001$), or F4 (Fibroscan®, AUROC = 0.888, $p < 0.0001$, ARFI-R, AUROC = 0.817, $p = 0.0002$). There was no significant difference in diagnostic accuracy between the Fibroscan® and ARFI-R methods ($p = 0.748$ for F0 vs. F1–4, $p = 0.512$ for F0–1 vs. F2–4, $p = 0.344$ for F0–2 vs. F3–4, and $p = 0.908$ for F0–3 vs. F4). *AUC* area under curve, *TPF* true positive fraction, *FPF* false positive fraction

Table 3 Diagnostic accuracy for the stages of fibrosis by Fibroscan® and ARFI-R (a) Total cases, (b) Viral, (c) Non-viral

	Fibroscan® ($n = 109$)			ARFI-R ($n = 113$)			p value Fibroscan® vs. ARFI-R
	AUC	Cut-off value	LR	AUC	Cut-off value	LR	
(a) Total							
F0 vs. F1–4	0.690	6.2	1.44	0.724	1.02	2.25	0.748
F0–1 vs. F2-4	0.891*	9.1	2.80	0.871*	1.30	2.37	0.512
F0–2 vs. F3–4	0.908*	11.6	3.96	0.890*	1.65	3.86	0.344
F0–3 vs. F4	0.888*	14.3	3.71	0.817*	1.88	3.52	0.908
	Fibroscan® ($n = 59$)			ARFI-R ($n = 59$)			p value Fibroscan® vs. ARFI-R
	AUC	Cut-off value	LR	AUC	Cut-off value	LR	
(b) Viral							
F0 vs. F1–4	NT	NT	NT	NT	NT	NT	NT
F0–1 vs. F2–4	0.887*	11.6	6.93	0.905*	1.40	2.90	0.239
F0–2 vs. F3–4	0.919*	11.6	4.72	0.923*	1.53	4.20	0.229
F0–3 vs. F4	0.924*	17.5	5.56	0.854*	1.88	4.55	0.217
	Fibroscan® ($n = 50$)			ARFI-R ($n = 54$)			p value Fibroscan® vs. ARFI-R
	AUC	Cut-off value	LR	AUC	Cut-off value	LR	
(c) Non-viral							
F0 vs. F1–4	0.677	6.25	1.73	0.730	1.02	2.27	0.724
F0–1 vs. F2–4	0.886*	9.1	3.2	0.842*	1.30	2.48	0.779
F0–2 vs. F3–4	0.882*	11.7	3.27	0.861*	1.45	2.48	0.715
F0–3 vs. F4	0.859*	14.3	3.41	0.793*	2.00	3.34	0.480

AUC area under curve, *LR* likelihood ratio, *NT* not tested

* $p < 0.05$ by χ^2 analysis

stage of fibrosis regardless of whether the cause was viral or non-viral. (Table 3b, c). For patients with non-viral etiology, a subanalysis was conducted to determine the accuracy of elastography measurements in patients with steatohepatitis. This was done because the fibrosis stage in patients with steatohepatitis should be assessed using a different scale (Brunt's classification) [13]. The numbers of patients with stages F0, F1, F2, F3, and F4 were 3, 13, 3, 5, and 7, respectively, by METAVIR classification, and 1, 5, 10, 8, and 7, respectively, by Brunt's classification. The AUROC values for Fibroscan® were 0.820 (F0 vs. F1–4), 0.913 (F0–1 vs. F2–4), 0.904 (F0–2 vs. F3–4), and 0.854 (F0–3 vs. F4) when using the METAVIR classification, and 0.963 (F0 vs. F1–4), 0.898 (F0–1 vs. F2–4), 0.913 (F0–2 vs. F3–4), and 0.854 (F0–3 vs. F4) with Brunt's classification. The AUROC values for ARFI-R were 0.820 (F0 vs. F1–4), 0.846 (F0–1 vs. F2–4), 0.868 (F0–2 vs. F3–4), and 0.738 (F0–3 vs. F4) using the METAVIR classification, and 0.867 (F0 vs. F1–4), 0.797 (F0–1 vs. F2–4), 0.846 (F0–2 vs. F3–4), and 0.738 (F0–3 vs. F4) using Brunt's classification. The accuracy for differentiation between F0 and F1 or higher stages improved when the stage of fibrosis was assessed by Brunt's classification, and thus, both Fibroscan® and ARFI accurately corresponded with fibrosis stage.

Effect of inflammation and steatosis on accuracy of elastography measurement

It has been reported that Fibroscan® data overestimate the pathological stage of fibrosis in samples with severe inflammation [14, 15]. Therefore, we compared the accuracy of elastography measurements according to the inflammatory activity in the liver biopsy specimens. The elastography values increased as the stage of fibrosis increased, regardless of the degree of inflammatory activity (Fig. 6a). As reported previously, among patients with mild fibrosis (F0 and F1), Fibroscan® values were significantly greater in patients with activity of A2–3 versus A0–1. However, these differences were not observed among patients with advanced fibrosis (F2, F3, and F4). The results of ARFI-R were similar to the Fibroscan® results, but no significant differences were observed according to the stage of fibrosis (data not shown). Therefore, the accuracy of these elastography measurements was re-estimated by ROC analysis (Table 4a). For Fibroscan®, the

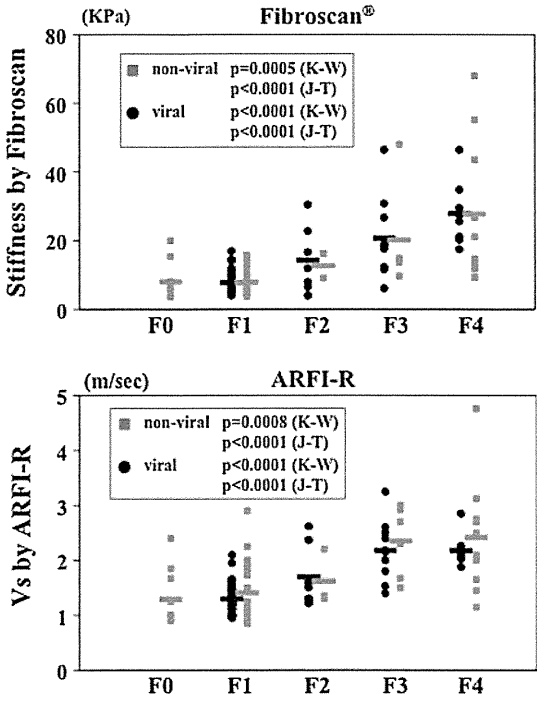

Fig. 5 The accuracy of elastography stratified according to the cause of liver damage. The *black circles* indicate elastography values for patients with viral hepatitis (viral) and the *gray squares* indicate values for patients with other (non-viral) etiologies. The *horizontal lines* indicate the average values for each stage. No patients with viral hepatitis were graded as showing F1. The values of both elastography measurements increased in proportion to the severity of fibrosis (Fibroscan®: (viral) $p < 0.0001$ by Kruskal–Wallis analysis, $p < 0.0001$ by Jonckheere–Terpstra test, (non-viral) $p = 0.0005$ by Kruskal–Wallis analysis, $p < 0.0001$ by Jonckheere–Terpstra test, ARFI-R: (viral) $p < 0.0001$ by Kruskal–Wallis analysis, $p < 0.0001$ by Jonckheere–Terpstra test, (non-viral) $p = 0.0008$ by Kruskal–Wallis analysis, $p < 0.0001$ by Jonckheere–Terpstra test), but there were no significant differences in the elastography values between the viral and non-viral patient groups at the same stages of fibrosis

AUROCs in differentiating F0 vs. F1–4 were 0.802 and 0.511; F0–1 vs. F2–4, the values were 0.899 and 0.861; F0–2 vs. F3–4, the values were 0.936 and 0.867, and F0–3 vs. F4, the values were 0.901 and 0.860 in relation to A0–1 and A2–3, respectively. For ARFI-R, the AUROCs for differentiating the stage of F1 or greater were 0.865 and 0.495; for F2 or greater, the values were 0.889 and 0.839, for F3 or greater, the values were 0.918 and 0.854; and for F4, the values were 0.874 and 0.735. These results indicate that, in patients with mild fibrosis, the accuracy for differentiating the stage of fibrosis decreased with stronger inflammatory activity. In addition, the inflammation only affected differentiation between F0 and F1–4 (Fibroscan® $p = 0.0480$, ARFI-R $p = 0.0082$), but there was no significant difference of diagnostic accuracy in other fibrosis stages by two-way analysis of variance.

Finally, we examined whether elastography measurements were influenced by hepatosteatosis. As shown in Fig. 6b, there were no significant differences between the values for patients with minimal steatosis (S0–1) and those with greater steatosis. The accuracy of elastography measurements was almost identical in the two groups (Table 4b). Moreover, the degree of steatosis did not affect the elastography measurements even when the data were submitted to two-way analysis of variance (data not shown).

Discussion

We herein describe the efficacy of ARFI elastography for the evaluation of liver fibrosis stage in patients with chronic liver damage of various etiologies. The ARFI technique was first introduced clinically to differentiate elastic regions in soft tissues by imaging [16]. Initially, this technology was used to detect tumors in soft tissues such as the liver and mammary gland [17]. Sarvazyan et al. [18] used tissue elastography in two volunteers to measure the velocity of oscillation of a wave generated by ARFI with US. Since then, the technology has evolved and it is now available as a simple machine equipped with US for transient elastography. ARFI technology enabled us to measure real-time liver stiffness during observation of the actual measuring site by B-mode US [21]. In addition to these advantages, tissue elastography with ARFI is very easy to perform and involves simply pushing a button during observation of the site of measurement or ROI. Among many indicators of liver fibrosis, such as elastography, serum fibrosis markers and formulae using various hematologic parameters [19, 20], Fibroscan® has been demonstrated to be the best way. In this study we evaluated the efficacy of ARFI elastography in comparison with that of Fibroscan®.

We attempted to measure both lobes of the liver in this study. The level of stiffness was always higher when we measured the left lobe, though the readings with both elastography methods were highly correlated with the stages of fibrosis. This difference may have been induced by direct pressure of the US probe on the liver when we measured the left lobe. When the right lobe is measured from the intercostal space, the US probe does not directly press on the liver because chest wall exists between US probe and the liver, but in the left lobe, the US probe directly presses on the liver via the abdominal wall. In acute liver damage, it has been reported that liver fibrosis is overestimated with the Fibroscan® method as compared with histology [14, 15]. Similar results were obtained in this study with ARFI, as well as with Fibroscan®; therefore, we excluded elastography values obtained from patients with acute liver damage from most analyses in this study. Moreover, it has been reported that histological

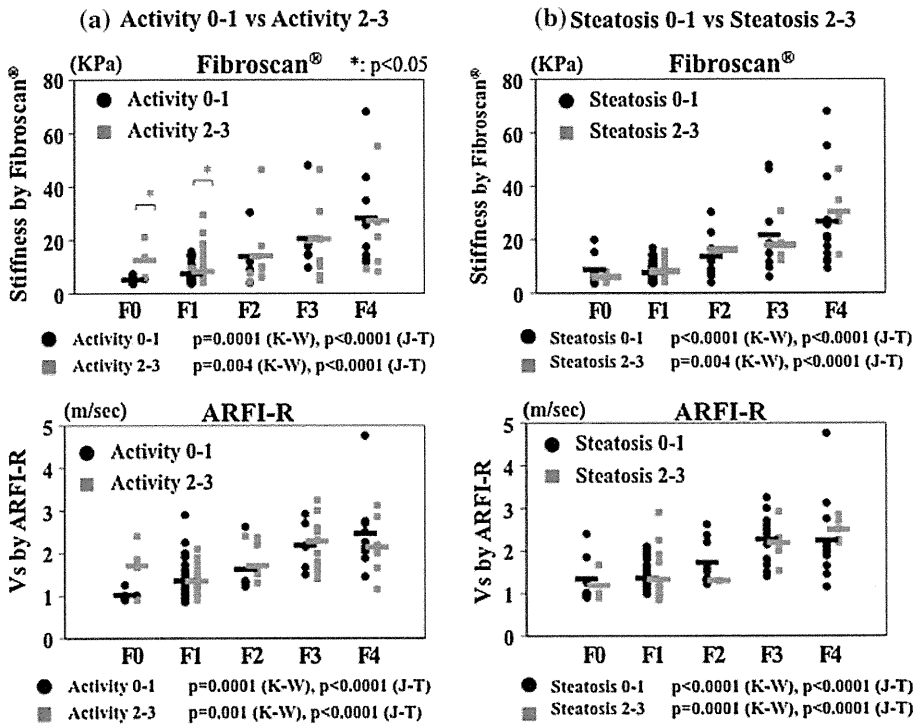

Fig. 6 Differences in elastography values according to the inflammatory activity or degree of steatosis in biopsy specimens. The elastography values increased in proportion to the severity of fibrosis, independently of the grade of inflammatory activity or steatosis. **a** In patients with mild fibrosis, the Fibroscan® values in those with high inflammatory activity (A2–3 *black circles*) were significantly greater than the values in patients with low activity (A0–1 *gray squares*) (F0: 5.1 ± 0.5 for A0–1 vs. 12.4 ± 6.5 for A2–3 $p = 0.0325$, F1: 7.3 ± 4.0 for A0–1 vs. 8.3 ± 3.1 for A2–3 $p = 0.0425$, by Wilcoxon analysis), but there were no significant differences among patients with greater than F2 grade fibrosis. ARFI-R values for patients with high inflammatory activity (A2–3) also tended to be greater than the values for patients with low activity (A0–1), but there were no significant differences at each stage of fibrosis. **b** Values obtained using either Fibroscan® or ARFI-R methods showed no differences between patients with mild steatosis (S0–1 *gray squares*) versus those with more severe steatosis (S2–3 *black circles*)

damage of the liver is uniform in viral hepatitis, which differs, in terms of histological heterogeneity, from findings in other chronic liver diseases such as autoimmune hepatitis and primary biliary cirrhosis. In the present study, measurement values by both ARFI and Fibroscan® increased in parallel with an increase in the stage of fibrosis in patients with viral liver damage as well as in those with non-viral liver damage, but the accuracy of differentiating the stage of fibrosis in patients with non-viral liver damage was slightly lower.

We found that the diagnostic power of differentiation between fibrosis stages with both methods always increased according to the increase in fibrosis stage. These data indicate that the diagnostic power of Fibroscan® and ARFI was almost equal, but the power for differentiating slight fibrosis was weak with both methods. In a meta-analysis of 50 studies with the Fibroscan® method, carried out predominantly in patients with chronic hepatitis C, the mean AUROCs for the diagnosis of significant fibrosis, severe fibrosis, and cirrhosis were 0.84, 0.89, and 0.94, respectively [22]. These findings suggest that transient elastography, performed with either Fibroscan® or ARFI, exhibits higher diagnostic power when fibrosis of the liver is more severe. In the present study, we also analyzed the elastography values by stratifying them according to the grade of inflammation or steatosis in liver biopsy specimens. As reported previously [14, 15], the elastography values in patients with more severe inflammation, (i.e., grade A2 and A3), overestimated the amount of liver fibrosis as compared with the histological findings, but the grade of steatosis did not affect these values. These tendencies were similar with both elastography methods. These factors should be considered when evaluating liver stiffness by tissue elastography.

Liver biopsy is considered the 'gold standard' for diagnosing chronic liver disease, grading necroinflammatory activity, and staging liver fibrosis. However, sampling error can lead to the underestimation of liver fibrosis, especially when biopsy specimens are small or fragmented [3, 4]. In the present study, the Fibroscan® values (20.5 kPa) and ARFI-R values (2.2 m/s) in patients with F3 stage fibrosis were higher than those described in previous reports [23–25]. The Fibroscan® value in our previous report was also lower (13.85 kPa) [8]. It may be difficult to